Mitochondrial Pyruvate Carrier Inhibition Initiates Metabolic Crosstalk to Stimulate Branched Chain Amino Acid Catabolism

Daniel Ferguson[1], Sophie J. Eichler[1], Nicole K.H. Yiew[1], Jerry R. Colca[2], Kevin Cho[3], Gary J. Patti[1,3,4], Kyle S. McCommis[5], Natalie M. Niemi[6], Brian N. Finck[1†]

[1]Department of Medicine, Center for Human Nutrition, Washington University in St. Louis.

[2]Department of Biomedical Sciences, Western Michigan University School of Medicine, Kalamazoo, MI; Cirius Therapeutics, Kalamazoo, MI

[3]Department of Chemistry, [4]Siteman Cancer Center, Washington University in St. Louis

[5]Department of Biochemistry & Molecular Biology, Saint Louis University School of Medicine.

[6]Department of Biochemistry and Molecular Biophysics, Washington University in St. Louis.

Running Title: Mitochondrial metabolic crosstalk

[†]Contact for Correspondence:
Brian N. Finck
660 S. Euclid Avenue,
Campus Box 8031,
St. Louis, MO 63110
bfinck@wustl.edu

ABSTRACT

The mitochondrial pyruvate carrier (MPC) has emerged as a therapeutic target for treating insulin resistance, type 2 diabetes, and nonalcoholic steatohepatitis (NASH). We evaluated whether MPC inhibitors (MPCi) might correct impairments in branched chain amino acid (BCAA) catabolism, which are predictive of developing diabetes and NASH. In a randomized, placebo-controlled trial of an MPCi (MSDC-0602K) in people with NASH (EMMINENCE; NCT02784444), MSDC-0602K treatment, which led to marked improvements in insulin sensitivity and diabetes, decreased plasma concentrations of BCAAs compared to baseline while placebo had no effect. The rate-limiting enzyme in BCAA catabolism is the mitochondrial branched chain ketoacid dehydrogenase (BCKDH), which is deactivated by phosphorylation. BCKDH phosphorylation was reduced in liver of obese, hepatocyte-specific MPC2 knockout (LS-Mpc2-/-) mice compared to wild-type controls. In multiple human hepatoma cell lines, MPCi markedly reduced BCKDH phosphorylation and stimulated branched chain keto acid catabolism. Mechanistically, the effects of MPCi could be mimicked by activating mitochondrial pyruvate oxidation and reversed by addition of mitochondrial-permeable methyl-pyruvate, suggesting that intramitochondrial pyruvate accumulation suppresses BCKDH activity. The effects of MPCi on BCKDH phosphorylation were mediated by the BCKDH phosphatase PPM1K, and MPCi treatment also reduced phosphorylation of PPM1K likely at a key serine residue near the substrate binding cleft. These data demonstrate novel cross talk between mitochondrial pyruvate and BCAA metabolism and suggest that MPC inhibition leads to lower plasma BCAA concentrations and BCKDH phosphorylation via the phosphatase PPM1K.

INTRODUCTION

The mitochondrial pyruvate carrier (MPC) has emerged as a therapeutic target for treating for treating metabolic disease including insulin resistance, type 2 diabetes, and nonalcoholic steatohepatitis (NASH) (1-5). The MPC is a heterodimeric complex in the inner mitochondrial membrane that is composed of two proteins, MPC1 and MPC2 (6, 7). Given that pyruvate is synthesized primarily in the cytosol while the enzymes that metabolize pyruvate (pyruvate carboxylase and pyruvate dehydrogenase (PDH)) are localized exclusively in the mitochondrial matrix, transport across the inner mitochondrial membrane is a critical step in the metabolism of this substrate. Pharmacologic inhibition or genetic deletion of the MPC in the liver has been shown to be beneficial in mouse models of insulin resistance, diabetes, and NASH (10-14). Mitochondrial pyruvate metabolism is required for high rates of flux of pyruvate into the gluconeogenic pathway, which is markedly increased in diabetes (8). However, there could be other molecular mechanisms mediating therapeutic effects that have yet to be identified.

In addition to the well-known effects on glucose homeostasis, insulin resistance and diabetes are also associated with perturbations in lipid and amino acid metabolism (8). For example, plasma concentrations of valine, leucine, and isoleucine, which are classified as branched chain amino acids (BCAAs), are increased in people with obesity and insulin resistance (9-13), and high plasma BCAA concentrations are predictive of future development of diabetes (14). Marked weight loss in people with obesity leads to reduced plasma BCAA concentrations (15, 16). Furthermore, dietary restriction of BCAAs in Zucker diabetic fatty (ZDF) rats (17) lowers plasma BCAAs and improves insulin sensitivity, suggesting that high BCAA concentrations play a causative role in the development of insulin resistance. Consistent with this, genome-wide association studies in humans have demonstrated that genetic variations in enzymes controlling BCAA metabolism are associated with increased BCAA concentrations and are also linked to the development of insulin resistance (18, 19). Strategies that correct accumulation of these bioactive amino acids may have value as therapeutic avenues for treating diabetes.

Circulating BCAA concentrations are regulated by dietary intake, rates of protein synthesis and proteolysis, and BCAA catabolism. To be oxidized, BCAAs are first reversibly converted to branched chain keto acids (BCKAs) by branched chain aminotransferases (BCAT). Next, BCKAs undergo oxidation that is catalyzed by the BCKA dehydrogenase (BCKDH) enzyme complex (E1, E2, and E3 subunits) localized in the mitochondrial matrix. BCKDH catalyzes a committed and rate-limiting step in BCAA catabolism (20). BCKDH activity is regulated by inhibitory phosphorylation of serine 293 of the

E1 alpha subunit (phospho-BCKDH), which is mediated by a BCKDH kinase (BDK). Conversely, BCKDH is activated by a protein phosphatase (PPM1K) that removes this covalent modification (20). Mechanistic studies conducted over the past several years have demonstrated that the phosphorylation of BCKDH is increased in the liver of rodent models of obesity/diabetes (*ob/ob* and ZDF rats) (21, 22), suggesting that impairments in BCKA catabolism may drive the accumulation of BCAAs in obesity. The increase in phospho-BCKDH content seems to be mediated by reduced PPM1K and increased BDK activity (22) and genetic or pharmacologic approaches to suppress BDK activity or overexpress PPM1K are effective at enhancing BCKA catabolism and improving glucose intolerance in rodent models of obesity (23).

In this work we examined the potential effects of MPC inhibition on BCAA metabolism and explored the molecular mechanisms involved. These studies unveiled interesting metabolic crosstalk between the mitochondrial metabolism of pyruvate and BCKAs. Moreover, these studies suggest that part of the metabolic benefit derived from MPC inhibition could be mediated by stimulating the catabolism of BCAAs.

METHODS

Study design. EMMINENCE [ClinicalTrials.gov Identifier: NCT02784444] was a randomized, double-blind evaluation of MSDC-0602K's safety and potential efficacy in patients with type 2 diabetes and liver injury, assessing 3 oral daily doses of MSDC-0602K (62.5 mg, 125 mg and 250 mg) or placebo given for 12 months to adult patients with biopsy-proven NASH, with fibrosis and without cirrhosis (3). The patients were stratified for the co-diagnosis of type 2 diabetes and severity of fibrosis. Approximately 50% of the patients were diabetic and approximately 60% had advanced fibrosis of F2 or F3. The primary efficacy endpoint was assessed at 12 months. In the EMMINENCE study, the effects of MSDC-0602K on liver histology and liver and glucose metabolism markers were tested in patients with NASH diagnosed by liver biopsy, with and without T2D. Plasma amino acids were determined using NMR-based amino acid quantification as described previously (24). The study was conducted in accordance with ICH GCP and all applicable regulatory requirements. Patients provided written informed consent prior to study participation. The protocol and consent forms were approved by relevant institutional review boards.

Animal Studies. All animal experiments were approved by the Institutional Animal Care and Use Committee of Washington University in St. Louis. Hepatocyte-specific MPC2 knockout (LS-Mpc2-/-)

and leptin receptor deficient (*db/db* LS-Mpc2-/-) mice were generated as previously described (1). Littermates that did not express Cre were used as controls in all studies. For high fat diet studies, mice were switched from standard chow to a 60 % high fat diet (Research Diets Inc, #D12492) at 6 weeks of age and were maintained on diet for 20 weeks. Prior to sacrifice for tissue and blood collection, mice were fasted for 5 h.

Glucose tolerance testing was performed after a 5 hour fast, then mice were injected i.p. with D-glucose (1 g/ kg body weight), after an initial blood glucose measurement (time = 0). Glucose was monitored at indicated time points with a handheld glucose meter (Contour Next, Bayer).

Cell culture experiments. Huh7 and HepG2 human hepatoma cells were maintained in in DMEM (Thermofisher Cat# 11965092) supplemented with 10% fetal bovine serum, pyruvate (1 mM), and Penicillin-Streptomycin (100 U/mL). For inhibitor studies, cells were treated overnight in serum-free culture media containing indicated treatments. The following day, cells were starved in DMEM containing no serum, glucose, or amino acids (MyBioSource Cat# MBS6120661) with indicated treatments for durations described in the text, and then harvested for protein.

All drugs were solubilized in DMSO and added at an equal volume to vehicle (DMSO), which was no more than 0.1% of volume in media. Reagents were obtained from the following companies: UK5099 (Cayman); 7ACC2 (Cayman); Zaprinast (Sigma); MSDC-0602K (Cirius Therapeutics); BT2 (Sigma); Methyl-pyruvate (Sigma); dichloroacetate (Sigma); Ketoisovaleric acid [1-^{14}C] sodium salt (American Radiolabeled Chemicals, ARC 3191). For siRNA experiments, Huh7 cells were transfected with Silencer™ Pre-Designed siRNAs (Thermofisher): Silencer™ Negative Control No. 1 siRNA (Cat# AM4611); Ppm1k$^{\#1}$ (Cat# AM16708; siRNA ID:127997); Ppm1k$^{\#2}$ (Cat# AM16708; siRNA ID:127999); BDK$^{\#1}$ (Cat# AM16708; siRNA ID:110905); or BDK$^{\#2}$ (Cat# AM16708; siRNA ID:140032) using Lipofectamine RNAiMAX Transfection Reagent (Thermofisher) according to manufacturer's instructions. After 48 hours, cells were treated as previously mentioned for inhibitor experiments. For transfection experiments, Huh7 cells were plated to ~50-70 % confluency. The following day, cells were transfected with either human PPM1K (WT), or a Ser248Ala PPM1K mutant, with a c-terminal FLAG tag in pcDNA3.1, using Lipofectamine 3000 (Thermofisher) according to manufacturer's instructions. After 48 hours, media was replaced with serum-free DMEM with indicated treatments as previously mentioned above.

cDNA plasmids. Human PPM1K (accession number BC037552) was cloned into a modified pcDNA3.1 vector carrying a short linker region (amino acid sequence AAAAEFGG) and a C-terminal

FLAG tag. The PPM1K open reading frame was amplified by PCR and cloned using the EcoRI and NotI restriction sites of the pcDNA3.1 multiple cloning site. The S248A mutation was generated using site directed mutagenesis using the following primers: forward 5' GTTTTGTAGCTTGGAATGCTTTGGGGCAGCCTCAC 3' and reverse 5' GTGAGGCTGCCCCAAAGCATTCCAAGCTACAAAAC 3'. All clones were validated using Sanger sequencing.

Co-Immunoprecipitation. Huh7 cells were transfected and treated as described above. After treatment, cells were harvested in lysis buffer (50 mM Tris-HCl (pH 7.4), 40 mM NaCl, 1 mM EDTA (pH 8.0), 0.5% Triton X-100 (v/v)) with added protease and phosphatase inhibitors (Thermofisher). Proteins were immunoprecipitated using Anti-FLAG® M2 Magnetic Beads (Millipore-Sigma) then subjected to western blotting.

BCKA oxidation assay. We performed BCKDH oxidation assays using methods similar to those used for palmitate oxidation, as previously described (25), with minor modifications. Huh7 cells were plated in 3.5 cm dishes at ~70-80% confluency. The following day, media was replaced with serum-free culture media with indicated treatments overnight. The following day, media was replaced with amino acid free media with inhibitors (as described above) and incubated for 1 hour. [^{14}C]-KIV was added (0.065 μCi), then the dish was quickly placed into an airtight CO_2 collection chamber (Fischer Nalgene® style 2118 jar, fitted with a rubber stopper (Kontes 774250-0014), and a center-well hanging bucket (Kimble 882320-0000) containing Whatman filter paper soaked with 50 μL benzothonium hydroxide (Sigma)). After 30 minutes at 37˚C, the reaction was terminated by 100 μL of 0.5 M H_2SO_4, injected using a syringe. [^{14}C]-CO_2 liberation was allowed to proceed for an additional 30 minutes on ice, then the center-well collection bucket was cut and put into a liquid scintillation vial. Production of [^{14}C]-CO_2 was determined via a scintillation counter and normalized to cellular protein, determined using DC protein assay (Bio-Rad).

Mouse plasma amino acid quantification. Amino acids were extracted from 20 μL of plasma with 200 μL of methanol containing leucine-d_3 (320 ng), isoleucine-$^{13}C_6$,^{15}N (160 ng), and valine-d_8 (400 ng) as internal standards for Leu, Ile, and Val, respectively. Quality control (QC) samples were prepared by pooling aliquots of study samples and injected every four study samples to monitor instrument performances throughout these analyses. The analysis of amino acids was performed on a Shimadzu 20AD HPLC system and a SIL-20AC autosampler coupled to 4000Qtrap mass spectrometer (AB Sciex) operated in positive multiple reaction monitoring (MRM) mode. Data processing was conducted with Analyst 1.6.3 (Applied

Biosystems). The relative quantification data for all analytes were presented as the peak ratio of each analyte to the internal standard.

Metabolomics extraction and LC/MS analysis of cell metabolites. Huh7 cells were given indicated treatments for 48 hours then metabolites were extracted as previously described (26). Briefly, media was removed and cells were washed three times with PBS and three times with HPLC-grade water. Subsequently, cells were quenched with ice cold HPLC-grade methanol, then scraped and transferred to Eppendorf tubes. Samples were dried in a SpeedVac for 2-6 h. Dried samples were reconstituted in 1 mL of ice cold methanol:acetonitrile:water (2:2:1), and subjected to three cycles of vortexing, freezing in liquid nitrogen, and 10 min of sonication at 25˚C. Next, samples were then stored at -20˚C for at least 1 h then centrifuged at 14,000 X g and 4˚C. Supernatants were transferred to new tubes and dried by SpeedVac for 2-5 h. Protein content of cell pellets was measuring using the BCA kit (ThermoFisher). After drying the supernatant, 1 mL of water:acetonitrile (1:2) was added per 2.5 mg of cell protein, determined in pellets obtained after extraction. Samples were subjected to two cycles of vortexing and 10 min of sonication at 25˚C. Next, samples were centrifuged at 14,000 X g and 4˚C for 10 min, transferred supernatant to LC vials, and stored at -80˚C until MS analysis.

Ultra-high-performance LC (UHPLC)/MS was performed with a ThermoScientific Vanquish Horizon UHPLC system interfaced with a ThermoScientific Orbitrap ID-X Tribrid Mass Spectrometer (Waltham, MA). Hydrophilic interaction liquid chromatography (HILIC) separation was accomplished by using a HILICON iHILIC-(P) Classic column (Tvistevagen, Umea, Sweden) with the following specifications: 100 mm 3 2.1 mm, 5 mm. Mobile-phase solvents were composed of A = 20 mM ammonium bicarbonate, 0.1% ammonium hydroxide (adjusted to pH 9.2), and 2.5 μM medronic acid in water:acetonitrile (95:5) and B = 2.5 μM medronic acid in acetonitrile:water (95:5). The column compartment was maintained at 45˚C for all experiments. The following linear gradient was applied at a flow rate of 250 μL min^{-1}: 0-1 min: 90% B, 1-12 min: 90-35% B, 12-12.5 min: 35-25% B, 12.5-14.5 min: 25% B. The column was re-equilibrated with 20 column volumes of 90% B. The injection volume was 2 μL for all experiments.

Data were collected with the following settings: spray voltage, -3.5 kV; sheath gas, 35; auxiliary gas, 10; sweep gas, 1; ion transfer tube temperature, 275˚C; vaporizer temperature, 300˚C; mass range, 67-1500 Da, resolution, 120,000 (MS1), 30,000 (MS/MS); maximum injection time, 100 ms; isolation window, 1.6 Da. LC/MS data were processed and analyzed with the open-source Skyline software (27).

Immunoblotting. Western blotting was performed as previously described (26) using RIPA lysis

buffer (Cell Signaling Technology) with added protease and phosphatase inhibitors (Thermofisher). For liver tissue, ~30 mg of liver was homogenized using a Tissuelyser. For *in vitro* experiments, cells were scraped in lysis buffer then briefly sonicated. Lysates were normalized to protein concentration, denatured and run on NuPAGE precast 4-12% Bis-Tris gels with MOPS buffer, and transferred to Immobilon PVDF. Antibodies were used from: Phospho-BCKDH-E1α Ser293 (Cell Signaling Technology (CST) 40368), BCKDH-E1α (CST 90198), MPC1 (CST 14462), MPC2 (CST 46141), H3 (CST 14269), HSP60 (CST 12165), β-Actin (CST 3700), Phospho-PDH α1 Ser293 (CST 31866), and PDH (CST 3205); BDK (sc-374425) and PPM1K (sc-514925); α-Tubulin (Sigma T8203); and DBT (Thermofisher #PA5-29727). Images were obtained using the Licor system with Image Studio Lite software. For separation of phosphorylated PPM1K, FUJIFILM Wako Pure Chemical Corporation SuperSep™ Phos-tag™ (50μmol/l), 7.5%, 17well, 100×100×6.6mm gels were used according to manufacturer's instructions using lysis buffer without EDTA.

Statistical Analyses. Figures were generated using GraphPad Prism Software version 9.0.1 for windows. Human data are presented as mean ± SD. All animal data and human data in Figure 1 are presented as the mean ±SEM. Statistical significance was calculated using an unpaired Student's t-test, two-way analysis of variance (ANOVA) with repeated measures, or one-way ANOVA with Tukey's multiple comparisons test, with a statistically significant difference defined as $p<0.05$.

RESULTS

MPCi treatment reduced plasma BCAA concentrations in people with NASH. Recently, a randomized, placebo-controlled, Phase IIB clinical trial of an MPCi (MSDC-0602K) in people with NASH (EMMINENCE; NCT02784444) was conducted (3). Patients were randomly assigned to placebo (n = 94), or 62.5 mg (n = 99), 125 mg (n = 98), or 250 mg (n = 101) of MSDC-0602K per day for 1 year. As previously reported (3), the two highest doses of MSDC-0602K led to lower insulin concentrations, while all three doses reduced glucose and increased adiponectin levels when compared to the placebo group (Table 1). We then examined BCAA concentrations in these patients by NMR. We found that the highest dose of MSDC-0602K led to lower concentrations of valine, leucine, isoleucine and total BCAA, while placebo had no effect (Figure 1). Interestingly, the low dose group had reduced valine levels, and a trend towards lower isoleucine ($p=0.0563$) and total BCAAs ($p=0.0501$). Finally, the high dose MSDC-0602K group had decreased levels of plasma alanine, a gluconeogenic amino acid, while plasma glycine, which has been shown to be lower in T2DM, trended to increase ($p=0.0863$)

(Supplemental Figure 1). Collectively, these data suggest that the MPCi MSDC-0602K reduces plasma BCAA concentrations in people with NASH.

Genetic deletion of the MPC in liver of mice reduces BCKDH phosphorylation. The rate-limiting enzyme in BCAA catabolism is the mitochondrial branched chain ketoacid dehydrogenase (BCKDH) that is deactivated by phosphorylation. To investigate the effect of MPC inhibition/deletion on BCKDH activation, we performed western blotting for hepatic phospho-BCKDH in wild-type and hepatocyte-specific MPC2 knockout (LS-Mpc2-/-) mice fed a high fat diet for 20 weeks. Not only did LS-Mpc2-/- mice have an improvement in glucose tolerance (Figure 2A), these mice had a 45% decrease in levels of hepatic phospho-BCKDH compared to wild-type mice (Figure 2B). We further tested this in a genetic model of obesity by crossing LS-Mpc2-/- mice on to the *db/db* background, which have previously been described to have lower blood glucose concentrations and improved glucose tolerance (1). The *db/db* mice had a substantial increase in liver phospho-BCKDH levels and loss of Mpc2-/- in hepatocytes slightly, but significantly, decreased BCKDH phosphorylation (Figure 2C). Plasma leucine, valine, and total BCAA levels were elevated in *db/db* mice, compared to lean controls, whereas only valine levels were elevated in LS-Mpc2-/- on the *db/db* background (Supplemental Figure 2). Collectively, these data demonstrate that hepatocyte-specific deletion of MPC2 leads to decreased BCKDH phosphorylation (indicative of increased activity) in both dietary and genetic models of obesity/hyperglycemia.

Inhibition of the MPC reduces BCKDH phosphorylation in human hepatoma cell lines. Next, we sought to determine if MPCi could affect BCKDH phosphorylation in an *in vitro* system. Using human hepatoma cell lines (Huh7 and HepG2), we tested several MPCi including the well-established UK5099, and more recently discovered 7ACC2, zaprinast, and MSDC-0602K. Overnight treatment of serum-starved hepatoma cells with the various MPCi resulted in substantial decreases in phospho-BCKDH, relative to vehicle-treated Huh7 cells (Figure 3A). 7ACC2 also reduced BCKDH phosphorylation in HepG2 cells (Supplemental Figure 3). Additionally, this effect was dose-dependent, with marked decreases in BCKDH phosphorylation being observed in the nanomolar (UK5099 and 7ACC2) and micromolar (MSDC-0602K) range (Figure 3B). These dose effects are consistent with the established potency of these compounds as MPCi (2, 28). Lastly, we performed a time-course study and saw observable decreases in phospho-BCKDH with as little as 30 minutes of MPCi treatment (Figure 3C). Taken together, these data indicate that various MPCi lead to reduced BCKDH phosphorylation.

Although phosphorylation of BCKDH is highly linked to activity (29), we also tested the effect of MPCi on BCKDH function more directly. We assessed rates of BCKA oxidation by measuring

conversion of radiolabeled ^{14}C-ketoisovaleric acid (ketovaline) into $^{14}CO_2$. Treatment of Huh7 cells with 7ACC2 lead to a significant 32% increase in BCKDH oxidation relative to vehicle (Figure 4B). Furthermore, we quantified metabolites from Huh7 cells treated with various MPCi and found trends toward increases in downstream BCAA catabolites including propionyl CoA and acetyl CoA (Figure 4C). We also observed substantial decreases in levels of various TCA intermediates including citrate, fumarate, and malate, which is consistent with a suppression of pyruvate entry into the TCA cycle (Figure 4C). Overall, these data suggest that MPCi lead to increased BCKDH activity and BCAA catabolism *in vitro*.

Intramitochondrial pyruvate enhances BCKDH phosphorylation. Previous studies have shown that pyruvate and glucose negatively regulate BCKDH activity in the perfused rat heart (30, 31). This effect can be reversed by treatment with dichloroacetate (DCA), which inhibits pyruvate dehydrogenase kinase to stimulate pyruvate oxidation. We hypothesized that MPCi could be preventing the accumulation of high intramitochondrial levels of pyruvate, thus avoiding the inhibitory effects of pyruvate on BCKDH activity. Addition of pyruvate to the media resulted in increased BCKDH phosphorylation (Figure 5A). Treatment with 7ACC2 or DCA mostly blocked the effects of added pyruvate and led to a substantial decrease in phospho-BCKDH with both vehicle and MPCi treatment (Figure 5A). To further investigate the hypothesis that intramitochondrial pyruvate was driving an increase in phospho-BCKDH, we treated cells with methyl-pyruvate, which can circumvent the MPC to enter the mitochondrion because its lipophilicity allows it to be membrane-permeable (32). Once again, we saw that the addition of pyruvate increased phospho-BCKDH levels and this was reduced with 7ACC2 treatment (Figure 5B). In contrast, supplementation with the membrane-permeable methyl-pyruvate blunted the effects of MPCi on BCKDH phosphorylation. Taken together, these data indicate that MPCi likely decreases intramitochondrial pyruvate levels, consequently preventing the inhibitory effects of pyruvate on BCKDH activity.

PPM1K mediates the effects of MPCi on BCKDH phosphorylation. BCKDH phosphorylation is controlled by a BCKDH kinase (BDK) and a corresponding phosphatase PPM1K (aka PP2Cm or PP2Ckappa) (20). To determine whether MPCi might be regulating BCKDH phosphorylation by inhibiting BDK, we tested whether MPCi had additive effects with BT2; a chemical inhibitor of BDK. As can be seen in Figure 6A, treatment with either a low or high dose of BT2 reduced phospho-BCKDH in vehicle-treated cells. However, MPCi treatment had an additive and quantitatively greater effect even with high dose BT2 (Figure 6A), suggesting that inhibition of BDK does not contribute to MPCi-

mediated effects on BCKDH phosphorylation. To confirm this, we used siRNA to selectively diminish expression of either PPM1K or BDK. Western blotting confirmed decreased protein expression of PPM1K or BDK with the respective siRNA (Figure 6B). MPCi-treatment yielded a comparable reduction in phospho-BCKDH levels in both control and BDK siRNA treated cells; again, suggesting a BDK-independent effect. In contrast, PPM1K siRNA markedly blunted the effects of MPCi on BCKDH phosphorylation (Figure 6B), suggesting that MPCi-induced effects on phospho-BCKDH are mediated via the PPM1K phosphatase.

MPC inhibition leads to reduced phosphorylation of PPM1K. Previous work has demonstrated that the addition of BCKAs, which lead to increased BCKDH activity, results in enhanced binding of PPM1K to the BCKDH complex via the E2 subunit (DBT) (33). We tested whether MPCi induced an increase in PPM1K binding to DBT by performing co-immunoprecipitation experiments in Huh7 cells overexpressing FLAG-tagged PPM1K. As shown in Figure 6C, we saw no appreciable difference in the interaction between PPM1K and DBT between vehicle and 7ACC2-treated cells.

PPM1K has been previously identified as a phospho-protein in several unbiased phosphoproteomic screens (34, 35). To determine if MPCi treatment altered PPM1K phosphorylation, we treated cells with either vehicle or 7ACC2, then separated them on Phos-Tag™ gels that distinguish phosphorylation status of proteins via altered mobility. Vehicle-treated cells had a greater proportion of the phosphorylated form of PPM1K, as indicated by the more intense signal on the upper band (Figure 6D). In contrast, cells treated with 7ACC2 displayed most signal in the lower band, indicating the majority of PPM1K was hypophosphorylated after MPCi treatment. Treatment with MPCi did not affect PPM1K protein abundance as assessed by performing western blotting using regular SDS-PAGE gels (Figure 6D, lower). In prior phospho-proteomic screens (34), serine 248 of PPM1K has emerged as a consensus phosphorylation site that is conserved between human and mouse PPM1K proteins and is in a highly homologous region of the protein (Figure 6E). Serine-248 was mutated to alanine (S248A) by site-directed mutagenesis of a cDNA encoding human PPM1K in an expression plasmid. These vectors were then transfected into Huh7 cells to overexpress either wild-type or S248A mutant PPM1K. When run on a Phos-Tag™ gel, S248A mutant protein migrated faster on the gel consistent with a less phosphorylated protein (Figure 6F). Moreover, the effect of 7ACC2 on Phos-Tag™ gel migration was abolished by the S248A mutation. These data suggest that MPC inhibition reduces PPM1K phosphorylation, likely at serine 248, and that this change in phosphorylation may mediate the effect of MPCi on BCKDH phosphorylation (Figure 6G).

DISCUSSION

In recent years, the MPC has demonstrated effectiveness for treating metabolic diseases such as insulin resistance, type 2 diabetes mellitus (T2DM), and NASH in both animal models and in clinical trials (1-5). Although plausible mechanisms of action for the effectiveness of MPCi in these diseases have been identified, other possibilities remain to be explored. In the current work, we investigated the possible effects of MPC inhibition on BCAA metabolism, which is dysregulated in insulin resistance and T2DM, and further dissected the mechanisms taking place. Herein we show that patients with NASH, treated with the MPCi MSDC-0602K, had marked reductions in plasma BCAA levels, which coincided with improvements in plasma glucose, insulin, and adiponectin concentrations. Mechanistically, we found that genetic or pharmacologic inhibition of the MPC leads to reduced phosphorylation of BCKDH that is likely secondary to diminished intramitochondrial pyruvate and mediated by the PPM1K phosphatase. Lastly, our data indicate that MPCi lead to decreased phosphorylation of PPM1K, likely at serine 248, to possibly enhance the activity of this BCKDH-regulating phosphatase. Collectively, our work indicates a novel mechanism whereby MPCi modulate the cross talk between mitochondrial pyruvate and BCAA metabolism, and enhance BCKDH activity via PPM1K to lower plasma BCAA concentrations.

Multiple metabolomic studies have demonstrated that plasma BCAA, and related metabolites, are highly correlated with insulin resistance, T2DM, and risk of future development of T2DM in humans (9-13). However, whether BCAA levels promote insulin resistance, or are simply a consequence of the disease, is still a matter of debate. Indeed, reports correlating elevated BCAA levels to increased serum insulin, in patients with obesity, suggested that elevated levels were likely a secondary manifestation of obesity since amino acid levels decreased upon weight loss (9, 36). In contrast, genome-wide association studies have linked genetic variations in enzymes that control BCAA metabolism (18, 19, 37), especially PPM1K (19), to plasma BCAA levels and insulin resistance and dietary restriction of BCAA in ZDF rats lowers plasma BCAAs and improves insulin sensitivity (17), suggesting that high BCAA concentrations play a causative role in the development of insulin resistance. Herein, we report that treatment with an insulin sensitizing MPCi lowers plasma BCAA in people with T2DM and in ND patients in association with marked reductions in plasma glucose and insulin concentrations. While the present studies cannot clarify the cause-and-effect relationship between BCAAs and insulin resistance in people, they are consistent with another study demonstrating that an insulin sensitizing agent and known MPCi, pioglitazone, also lowers plasma BCAAs in people with NASH (38).

Circulating BCAA are increased in Zucker diabetic fatty rats (ZDF), which is believed to be mediated by reduced levels of PPM1K and increased hepatic BDK activity, which leads to increased phospho-BCKDH and impaired BCKA oxidation (17, 21, 22). In contrast, diet-induced obese mice were found to have no change in plasma BCAA (39). This may be explained by species differences in the regulation of BDK, since mice lack a carbohydrate response element binding protein (ChREBP) binding site in the BDK promoter that is present in rats and humans (23). However, there are some reports that mice with leptin or leptin receptor mutations exhibit elevated plasma BCAA concentrations (21, 22, 26). In the present study, we found that *db/db* mice exhibit increased hepatic phospho-BCKDH, which was reduced in *db/db* LS-Mpc2-/-; however, we did not see a dramatic decrease in circulating BCAAs between fl/fl and LS-Mpc2-/- on the *db/db* background (Supplemental Figure 2). It is possible that the effects on BCKDH phosphorylation, seen with hepatocyte-specific *Mpc2* deletion, are not great enough to enhance BCKA catabolism to a degree that results in reduced circulating BCAAs. There is also the possibility that the effects of pharmacologic MPCi on BCAAs are more dramatic because they are not liver-specific and could enhance BCKA oxidation in other organs that have high rates of BCKA catabolism.

The present findings describe metabolic crosstalk between mitochondrial pyruvate and BCKA metabolism. Our model suggests that high intramitochondrial pyruvate abundance leads to increased phospho-BCKDH. This is supported by evidence that supplementation of pyruvate increases phospho-BCKDH, but that this can be counteracted by MPCi or enhancing pyruvate oxidation with DCA. This model is also supported by our observation that membrane permeable methyl pyruvate overcame the effects of MPCi. These effects on BCKDH covalent modification are consistent with biochemical data generated many years ago by the Olson group (30, 31). In those studies, they found that addition of pyruvate suppressed ^{14}C-BCKA oxidation in heart and that DCA and an early MPCi (α-cyanocinnamate) could prevent the effects of exogenous pyruvate on BCKA oxidation (30). At that time, the regulation of BCKDH activity by phosphorylation had yet to be discovered and was therefore not assessed. The present studies are quite consistent with these historic findings and add additional mechanistic insight including demonstration that the effects of pyruvate and MPCi are likely mediated by the phosphorylation status of BCKDH and require PPM1K activity.

The mitochondrial phosphatase PPM1K is known to bind to the E2 subunit of the BCKDH complex, and dephosphorylate the E1 alpha subunit at serine 293 to increase BCKDH activity (33). Mutations in the gene encoding PPM1K lead to maple syrup urine disease in people, which is

characterized by high urinary excretion of BCAAs and BCKAs due to impaired BCKA oxidation (40). The gene encoding PPM1K is transcriptionally regulated in HepG2 cells and is downregulated in media without BCAA (41), but we saw no effect of MPCi on the abundance of PPM1K. Prior work has suggested that the protein-protein interaction between the BCKDH and PPM1K can be enhanced by exogenous supplementation of BCKAs (33). In the present study, we found that MPCi did not increase the binding of PPM1K to the BCKDH E2 subunit. Instead, our data suggest MPCi treatment led to reduced PPM1K phosphorylation in Huh7 cells. With the advent of high throughput phosphoproteomics, serine 248 of PPM1K has been identified as a phosphorylation site in analyses of hepatic mitochondrial proteins (34). A mutant PPM1K protein with an S248A mutation was resistant to the effects of MPCi on PhosTAG^{TM} gel mobility, suggesting that this could be an important site of covalent modification in response to MPCi. Though the functional effects of this modification remain to be determined, work on the crystal structure of PPM1K suggests that serine 248 is localized near the active site cleft of PPM1K (42), which could affect the intrinsic phosphatase activity of this enzyme. Available data indicate an increase in PPM1K serine 248 phosphorylation in 10-week-old *ob/ob* mice, as well as acute downregulation of this phosphosite in after refeeding fasted mice (34) (mitomod.biochem.wisc.edu). These changes, and the data presented herein, would be consistent with the phosphorylation of serine 248 having an inhibitory effect on PPM1K activity, but this still needs to be experimentally determined.

To conclude, we show that use of the MPCi MSDC-0602K, in people with NASH, led to marked improvement in insulin sensitivity and glycemia, which was accompanied by substantial decreases in circulating BCAA levels. Furthermore, phosphorylation of BCKDH, which inactivates the rate-limiting enzyme in BCAA catabolism, was decreased in the liver of LS-Mpc2-/- mice and human hepatoma cell lines treated with MPCi. Activation of pyruvate oxidation mimicked the effect of MPCi that could be reversed by the addition of mitochondrial membrane-permeable methyl-pyruvate, suggesting that MPCi may enhance BCKDH activity by reducing intramitochondrial pyruvate accumulation. Lastly, we showed that the effects of MPCi were mediated by the phosphatase PPM1K, possibly through a novel mechanism involving phosphorylation at serine 248. Collectively, these data reveal cross talk between BCAA metabolism and mitochondrial pyruvate, and provide evidence that inhibition of the MPC leads to reduced circulating BCAA levels and hepatic BCKDH phosphorylation via the phosphatase PPM1K.

ACKNOWLEDGMENTS

This work was funded by NIH grants R01 DK104735 and R01 DK117657 (to B.N.F.). The Core services of the Diabetes Research Center (P30 DK020579), Digestive Diseases Research Cores Center (P30 DK052574), and the Nutrition Obesity Research Center (P30 DK56341) at the Washington University School of Medicine also supported this work. D.F was supported by a training grant (T32 DK007120). N.K.H.Y. was supported by a training grant (T32 HL134635). K.S.M. was supported by (R00 HL136658). Some metabolic analyses were supported by NIH grant R35 ES028365 (to G.J.P.). The Washington University Metabolomics Facility conducted mouse plasma metabolomic analyses. The authors would like to thank Margery A. Connelly (LabCorp) for NMR-based analysis of amino acids in people.

DISCLOSURES

BNF is a shareholder and a member of the Scientific Advisory Board for Cirius Therapeutics, which is developing an MPC modulator for treating nonalcoholic steatohepatitis. JRC is the co-founder and part owner of Metabolic Solutions Development and Cirius Therapeutics which are developing clinical candidates including this class of potential therapeutics.

FIGURE LEGENDS

Figure 1. *MPCi treatment reduced plasma BCAA concentrations in people with NASH*. Change in the levels of fasting BCAA from baseline, after 12 months with indicated treatments (Mean and SE; ANOVA for dose versus placebo *p<0.05, **p<0.01)

Figure 2. *Genetic deletion of the MPC in liver of mice reduces BCKDH phosphorylation*. A and B, WT and LS-Mpc2-/- mice were fed a 60% high fat diet for 20 weeks. (A) Following a 5-hour fast glucose tolerance was assessed (n=13-19). (B) Representative western blot images of hepatic protein expression, with pBCKDH-S293/BCKDH ratio determined by densitometric analysis of band intensity (n=3-4). (C) Representative western blot images of hepatic protein expression in Mpc2fl/fl and LS-Mpc2-/- (KO) mice that were crossed into the db/db background, with pBCKDH-S293/BCKDH ratio determined by densitometric analysis of band intensity (n=3-4). All data are expressed as mean ± SEM. *p<0.05, **p<0.01.

Figure 3. *Inhibition of the MPC reduces BCKDH phosphorylation in human hepatoma cell lines*. Representative western blots of pBCKDH-S293, BCKDH, and α-Tubulin. (A) Huh7 cells were treated overnight with MPCi Veh (DMSO), UK-5099 (1 μM), 7ACC2 (1 μM), Zaprinast (Zap, 10 μM), and MSDC-0602K (lo, 10 μM; hi, 30 μM). (B) Cells were treated overnight with indicated concentration of MPCi. (C) Veh or 7ACC2 (2.5 μM) was added at the indicated time points before harvested for western blotting.

Figure 4. *BCKDH oxidation and BCAA catabolism are increased with MPC inhibition*. (A) Schematic showing the oxidative decarboxylation of BCKA, releasing CO_2, by BCKDH that is regulated via phosphorylation by BDK, or dephosphorylation by PPM1K. (B) BCKDH oxidation assay performed in Huh7 cells treated with either Veh or 7ACC2 (2.5 μM). (C) Analysis of metabolites performed after cells treated for 48 hours with either Veh (DMSO), UK-5099 (2.5 μM), 7ACC2 (2.5 μM), or MSDC-0602K (10 μM) for 48 hours. All data are expressed as mean ± SEM. *p<0.05, **p<0.01, ****p<0.0001.

Figure 5. *Intramitochondrial pyruvate enhances BCKDH phosphorylation*. (A) Cells were treated with Veh or 7ACC2 (2.5 μM), in the absence or presence of pyruvate (1 mM) or dichloroacetate (DCA, 20

mM) overnight. (B) Cells were treated with Veh or 7ACC2 (2.5 μM), in the absence or presence of pyruvate (10 mM) or methyl-pyruvate (10 mM) overnight.

Figure 6. *PPM1K mediates the effects of MPCi on BCKDH phosphorylation and MPC inhibition leads to reduced phosphorylation of PPM1K*. (A) Cells were treated with Veh or MPCi, in the absence or presence of the BDK inhibitor BT2 overnight, at indicated concentrations. (B) Cells were transfected with indicated siRNA, then 48 hours later were treated with either Veh or 7ACC2 overnight. (C) Cells were transfected with Human FLAG-tagged PPM1K, then treated with either Veh or 7ACC2 (2.5 μM) overnight and harvested for co-immunoprecipitation. (D) Cells were treated with Veh or 7ACC2 (2.5 μM) overnight, and separated using either PhosTag™ gels (Top) or normal SDS-PAGE (Bottom) and subjected to western blotting. (E) Sequence alignment surrounding serine 248 or both human and mouse PPM1K (phosphosite.org). (F) Cells were transfected with either human PPM1K (WT), or a Ser248Ala PPM1K mutant (S248A). After 48 hours, cells were treated with either Veh or 7ACC2 (2.5 μM) overnight and harvested for separation using PhosTag™ gels. (G) Schematic summarizing that MPCi induce a dephosphorylation of the phosphatase PPM1K, possibly enhancing phosphatase activity that reduces BCKDH phosphorylation leading to an increase in BCAA catabolism.

Supplemental Figure 1. *MPCi treatment alters amino acid concentrations in people with NASH*. Change in the levels of fasting alanine and glycine from baseline, after 12 months with indicated treatments (Mean and SE; ANOVA for dose versus placebo *p<0.05).

Supplemental Figure 2. *Circulating BCAAs in db/db mice with genetic deletion of the MPC in liver of db/db mice.* Relative levels of circulating BCAAs in Mpc2fl/fl and LS-Mpc2-/- (KO) mice that were crossed into the *db/db* background. All data are expressed as mean ± SEM. *p<0.05, **p<0.01 relative to *db/+*, fl/fl group.

Supplemental Figure 3. *Inhibition of the MPC reduces BCKDH phosphorylation in human hepatoma cell lines.* Representative western blots of pBCKDH-S293, BCKDH, and H3 in HepG2 cells treated overnight with Veh (DMSO) or 7ACC2 (1 μM).

.

References

1. McCommis KS, Chen Z, Fu X, McDonald WG, Colca JR, Kletzien RF, et al. Loss of Mitochondrial Pyruvate Carrier 2 in the Liver Leads to Defects in Gluconeogenesis and Compensation via Pyruvate-Alanine Cycling. *Cell metabolism.* 2015;22(4):682-94.
2. McCommis KS, Hodges WT, Brunt EM, Nalbantoglu I, McDonald WG, Holley C, et al. Targeting the mitochondrial pyruvate carrier attenuates fibrosis in a mouse model of nonalcoholic steatohepatitis. *Hepatology.* 2017;65(5):1543-56.
3. Harrison SA, Alkhouri N, Davison BA, Sanyal A, Edwards C, Colca JR, et al. Insulin sensitizer MSDC-0602K in non-alcoholic steatohepatitis: A randomized, double-blind, placebo-controlled phase IIb study. *Journal of hepatology.* 2020;72(4):613-26.
4. Gray LR, Sultana MR, Rauckhorst AJ, Oonthonpan L, Tompkins SC, Sharma A, et al. Hepatic Mitochondrial Pyruvate Carrier 1 Is Required for Efficient Regulation of Gluconeogenesis and Whole-Body Glucose Homeostasis. *Cell metabolism.* 2015;22(4):669-81.
5. Rauckhorst AJ, Gray LR, Sheldon RD, Fu X, Pewa AD, Feddersen CR, et al. The mitochondrial pyruvate carrier mediates high fat diet-induced increases in hepatic TCA cycle capacity. *Molecular metabolism.* 2017;6(11):1468-79.
6. Herzig S, Raemy E, Montessuit S, Veuthey JL, Zamboni N, Westermann B, et al. Identification and functional expression of the mitochondrial pyruvate carrier. *Science.* 2012;336(6090):93-6.
7. Bricker DK, Taylor EB, Schell JC, Orsak T, Boutron A, Chen YC, et al. A mitochondrial pyruvate carrier required for pyruvate uptake in yeast, Drosophila, and humans. *Science.* 2012;337(6090):96-100.
8. Petersen MC, and Shulman GI. Mechanisms of Insulin Action and Insulin Resistance. *Physiological reviews.* 2018;98(4):2133-223.
9. Felig P, Marliss E, and Cahill GF, Jr. Plasma amino acid levels and insulin secretion in obesity. *The New England journal of medicine.* 1969;281(15):811-6.
10. Thalacker-Mercer AE, Ingram KH, Guo F, Ilkayeva O, Newgard CB, and Garvey WT. BMI, RQ, diabetes, and sex affect the relationships between amino acids and clamp measures of insulin action in humans. *Diabetes.* 2014;63(2):791-800.
11. Palmer ND, Stevens RD, Antinozzi PA, Anderson A, Bergman RN, Wagenknecht LE, et al. Metabolomic profile associated with insulin resistance and conversion to diabetes in the Insulin Resistance Atherosclerosis Study. *The Journal of clinical endocrinology and metabolism.* 2015;100(3):E463-8.
12. Newgard CB, An J, Bain JR, Muehlbauer MJ, Stevens RD, Lien LF, et al. A branched-chain amino acid-related metabolic signature that differentiates obese and lean humans and contributes to insulin resistance. *Cell metabolism.* 2009;9(4):311-26.
13. Menni C, Fauman E, Erte I, Perry JR, Kastenmüller G, Shin SY, et al. Biomarkers for type 2 diabetes and impaired fasting glucose using a nontargeted metabolomics approach. *Diabetes.* 2013;62(12):4270-6.
14. Wang TJ, Larson MG, Vasan RS, Cheng S, Rhee EP, McCabe E, et al. Metabolite profiles and the risk of developing diabetes. *Nature medicine.* 2011;17(4):448-53.
15. Laferrère B, Reilly D, Arias S, Swerdlow N, Gorroochurn P, Bawa B, et al. Differential metabolic impact of gastric bypass surgery versus dietary intervention in obese diabetic subjects despite identical weight loss. *Science translational medicine.* 2011;3(80):80re2.

16. Shah SH, Crosslin DR, Haynes CS, Nelson S, Turer CB, Stevens RD, et al. Branched-chain amino acid levels are associated with improvement in insulin resistance with weight loss. *Diabetologia.* 2012;55(2):321-30.
17. White PJ, Lapworth AL, An J, Wang L, McGarrah RW, Stevens RD, et al. Branched-chain amino acid restriction in Zucker-fatty rats improves muscle insulin sensitivity by enhancing efficiency of fatty acid oxidation and acyl-glycine export. *Molecular metabolism.* 2016;5(7):538-51.
18. Wang Q, Holmes MV, Davey Smith G, and Ala-Korpela M. Genetic Support for a Causal Role of Insulin Resistance on Circulating Branched-Chain Amino Acids and Inflammation. *Diabetes Care.* 2017;40(12):1779-86.
19. Lotta LA, Scott RA, Sharp SJ, Burgess S, Luan J, Tillin T, et al. Genetic Predisposition to an Impaired Metabolism of the Branched-Chain Amino Acids and Risk of Type 2 Diabetes: A Mendelian Randomisation Analysis. *PLoS medicine.* 2016;13(11):e1002179.
20. Neinast M, Murashige D, and Arany Z. Branched Chain Amino Acids. *Annual review of physiology.* 2019;81:139-64.
21. She P, Van Horn C, Reid T, Hutson SM, Cooney RN, and Lynch CJ. Obesity-related elevations in plasma leucine are associated with alterations in enzymes involved in branched-chain amino acid metabolism. *American journal of physiology Endocrinology and metabolism.* 2007;293(6):E1552-63.
22. Lian K, Du C, Liu Y, Zhu D, Yan W, Zhang H, et al. Impaired adiponectin signaling contributes to disturbed catabolism of branched-chain amino acids in diabetic mice. *Diabetes.* 2015;64(1):49-59.
23. White PJ, McGarrah RW, Grimsrud PA, Tso SC, Yang WH, Haldeman JM, et al. The BCKDH Kinase and Phosphatase Integrate BCAA and Lipid Metabolism via Regulation of ATP-Citrate Lyase. *Cell metabolism.* 2018;27(6):1281-93.e7.
24. Wolak-Dinsmore J, Gruppen EG, Shalaurova I, Matyus SP, Grant RP, Gegen R, et al. A novel NMR-based assay to measure circulating concentrations of branched-chain amino acids: Elevation in subjects with type 2 diabetes mellitus and association with carotid intima media thickness. *Clinical biochemistry.* 2018;54:92-9.
25. Helsley RN, Varadharajan V, Brown AL, Gromovsky AD, Schugar RC, Ramachandiran I, et al. Obesity-linked suppression of membrane-bound O-acyltransferase 7 (MBOAT7) drives non-alcoholic fatty liver disease. *eLife.* 2019;8.
26. Martino MR, Gutiérrez-Aguilar M, Yiew NKH, Lutkewitte AJ, Singer JM, McCommis KS, et al. Silencing alanine transaminase 2 in diabetic liver attenuates hyperglycemia by reducing gluconeogenesis from amino acids. *Cell reports.* 2022;39(4):110733.
27. Adams KJ, Pratt B, Bose N, Dubois LG, St John-Williams L, Perrott KM, et al. Skyline for Small Molecules: A Unifying Software Package for Quantitative Metabolomics. *Journal of proteome research.* 2020;19(4):1447-58.
28. Hodges WT, Jarasvaraparn C, Ferguson D, Griffett K, Gill LE, Chen Y, et al. Mitochondrial pyruvate carrier inhibitors improve metabolic parameters in diet-induced obese mice. *The Journal of biological chemistry.* 2022;298(2):101554.
29. Paxton R, and Harris RA. Isolation of rabbit liver branched chain alpha-ketoacid dehydrogenase and regulation by phosphorylation. *The Journal of biological chemistry.* 1982;257(23):14433-9.
30. Waymack PP, DeBuysere MS, and Olson MS. Studies on the activation and inactivation of the branched chain alpha-keto acid dehydrogenase in the perfused rat heart. *The Journal of biological chemistry.* 1980;255(20):9773-81.

31. Buxton DB, and Olson MS. Regulation of the branched chain alpha-keto acid and pyruvate dehydrogenases in the perfused rat heart. *The Journal of biological chemistry.* 1982;257(24):15026-9.
32. Nishida N, Yasui H, Nagane M, Yamamori T, and Inanami O. 3-Methyl pyruvate enhances radiosensitivity through increasing mitochondria-derived reactive oxygen species in tumor cell lines. *Journal of radiation research.* 2014;55(3):455-63.
33. Lu G, Sun H, She P, Youn JY, Warburton S, Ping P, et al. Protein phosphatase 2Cm is a critical regulator of branched-chain amino acid catabolism in mice and cultured cells. *The Journal of clinical investigation.* 2009;119(6):1678-87.
34. Grimsrud PA, Carson JJ, Hebert AS, Hubler SL, Niemi NM, Bailey DJ, et al. A quantitative map of the liver mitochondrial phosphoproteome reveals posttranslational control of ketogenesis. *Cell metabolism.* 2012;16(5):672-83.
35. Humphrey SJ, Yang G, Yang P, Fazakerley DJ, Stöckli J, Yang JY, et al. Dynamic adipocyte phosphoproteome reveals that Akt directly regulates mTORC2. *Cell metabolism.* 2013;17(6):1009-20.
36. Yoshino M, Kayser BD, Yoshino J, Stein RI, Reeds D, Eagon JC, et al. Effects of Diet versus Gastric Bypass on Metabolic Function in Diabetes. *The New England journal of medicine.* 2020;383(8):721-32.
37. Mahendran Y, Jonsson A, Have CT, Allin KH, Witte DR, Jørgensen ME, et al. Genetic evidence of a causal effect of insulin resistance on branched-chain amino acid levels. *Diabetologia.* 2017;60(5):873-8.
38. Kalavalapalli S, Bril F, Koelmel JP, Abdo K, Guingab J, Andrews P, et al. Pioglitazone improves hepatic mitochondrial function in a mouse model of nonalcoholic steatohepatitis. *American journal of physiology Endocrinology and metabolism.* 2018;315(2):E163-e73.
39. Lee J, Vijayakumar A, White PJ, Xu Y, Ilkayeva O, Lynch CJ, et al. BCAA Supplementation in Mice with Diet-induced Obesity Alters the Metabolome Without Impairing Glucose Homeostasis. *Endocrinology.* 2021;162(7).
40. Oyarzabal A, Martínez-Pardo M, Merinero B, Navarrete R, Desviat LR, Ugarte M, et al. A novel regulatory defect in the branched-chain α-keto acid dehydrogenase complex due to a mutation in the PPM1K gene causes a mild variant phenotype of maple syrup urine disease. *Human mutation.* 2013;34(2):355-62.
41. Zhou M, Lu G, Gao C, Wang Y, and Sun H. Tissue-specific and nutrient regulation of the branched-chain α-keto acid dehydrogenase phosphatase, protein phosphatase 2Cm (PP2Cm). *The Journal of biological chemistry.* 2012;287(28):23397-406.
42. Dolatabad MR, Guo LL, Xiao P, Zhu Z, He QT, Yang DX, et al. Crystal structure and catalytic activity of the PPM1K N94K mutant. *Journal of neurochemistry.* 2019;148(4):550-60.

Figure 1

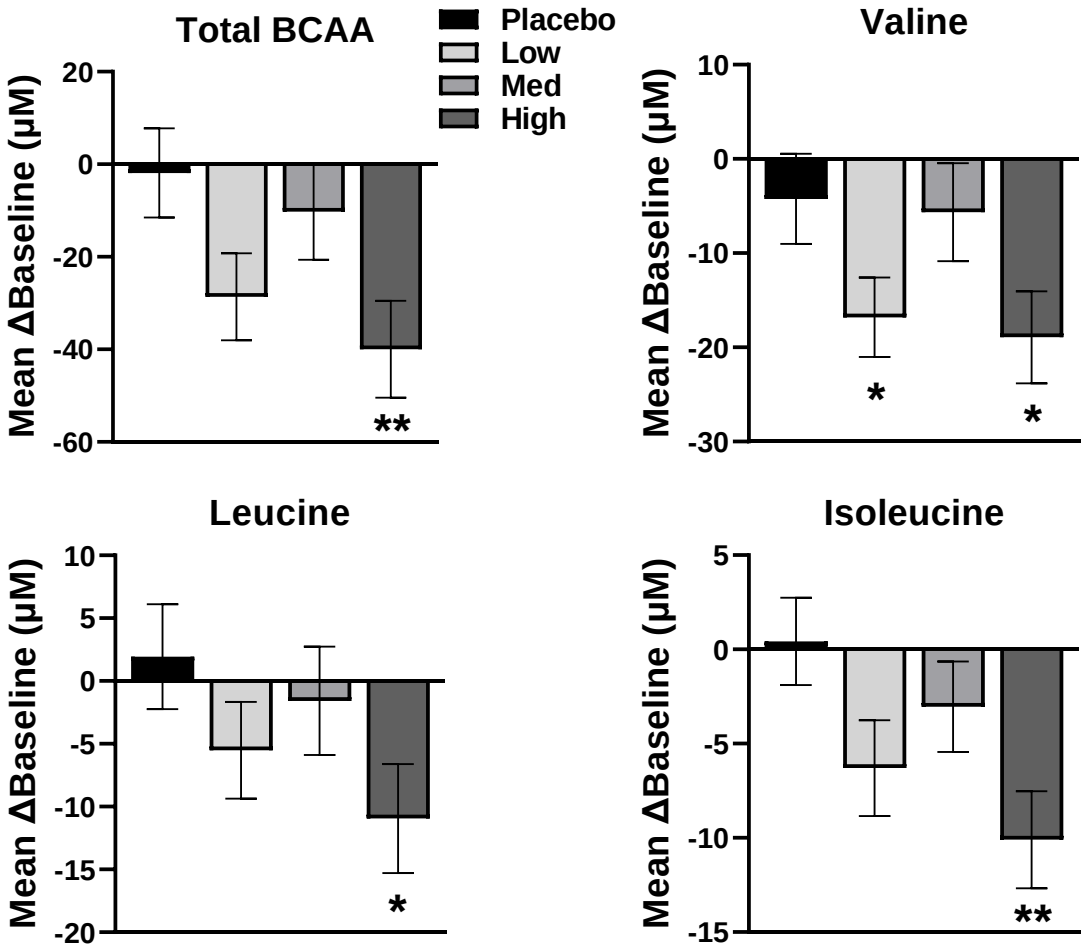

Figure 2

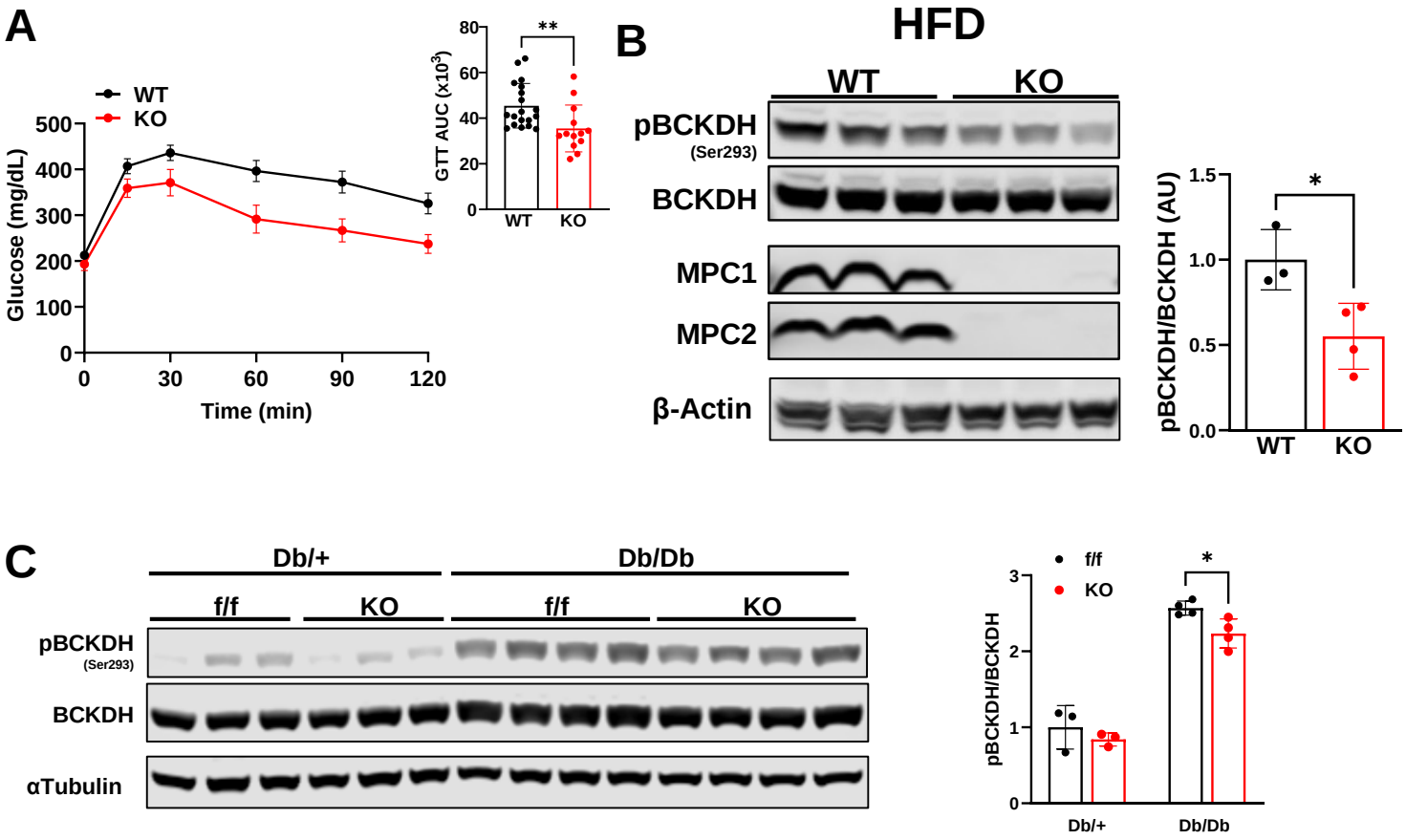

Figure 3

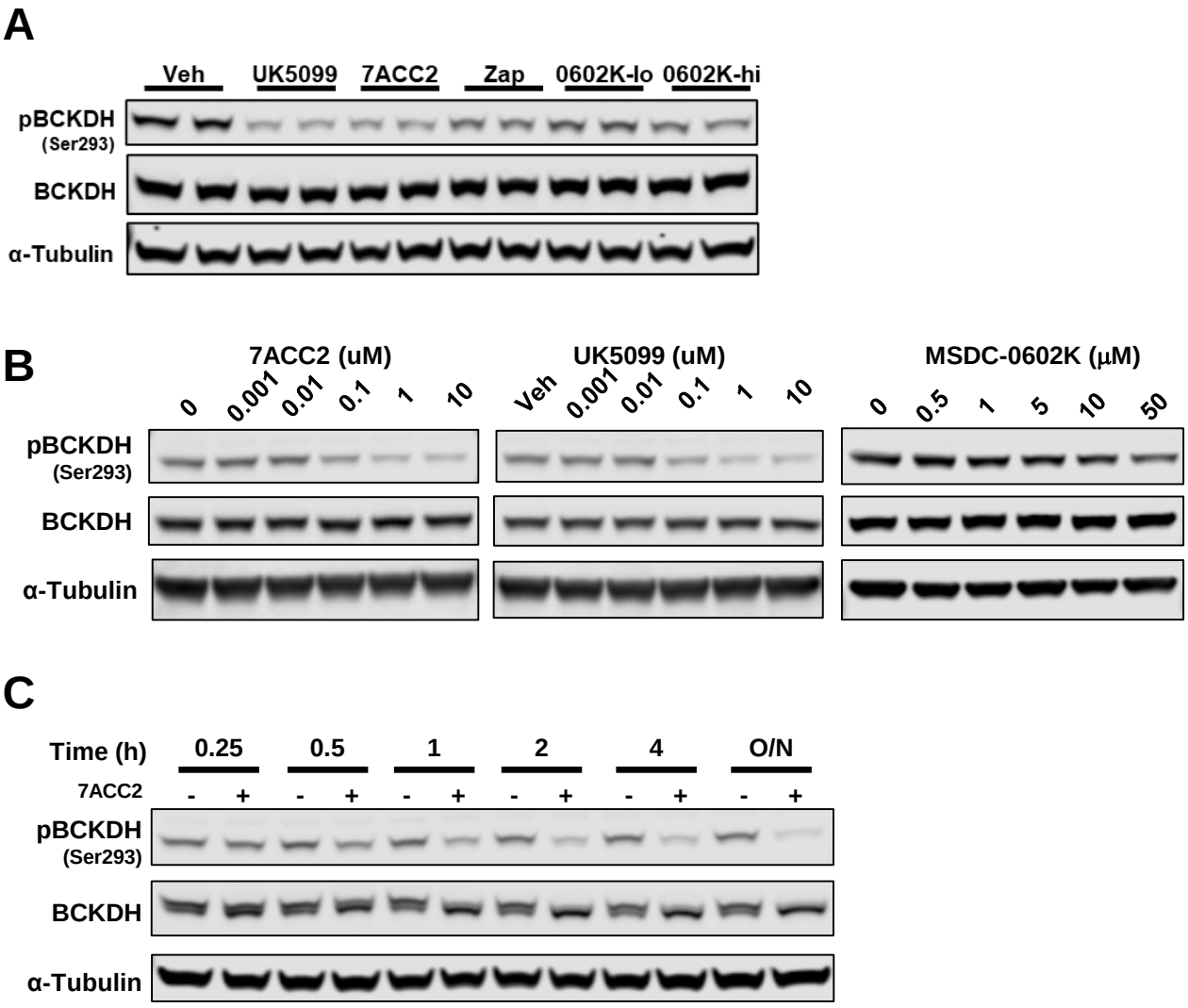

Figure 4

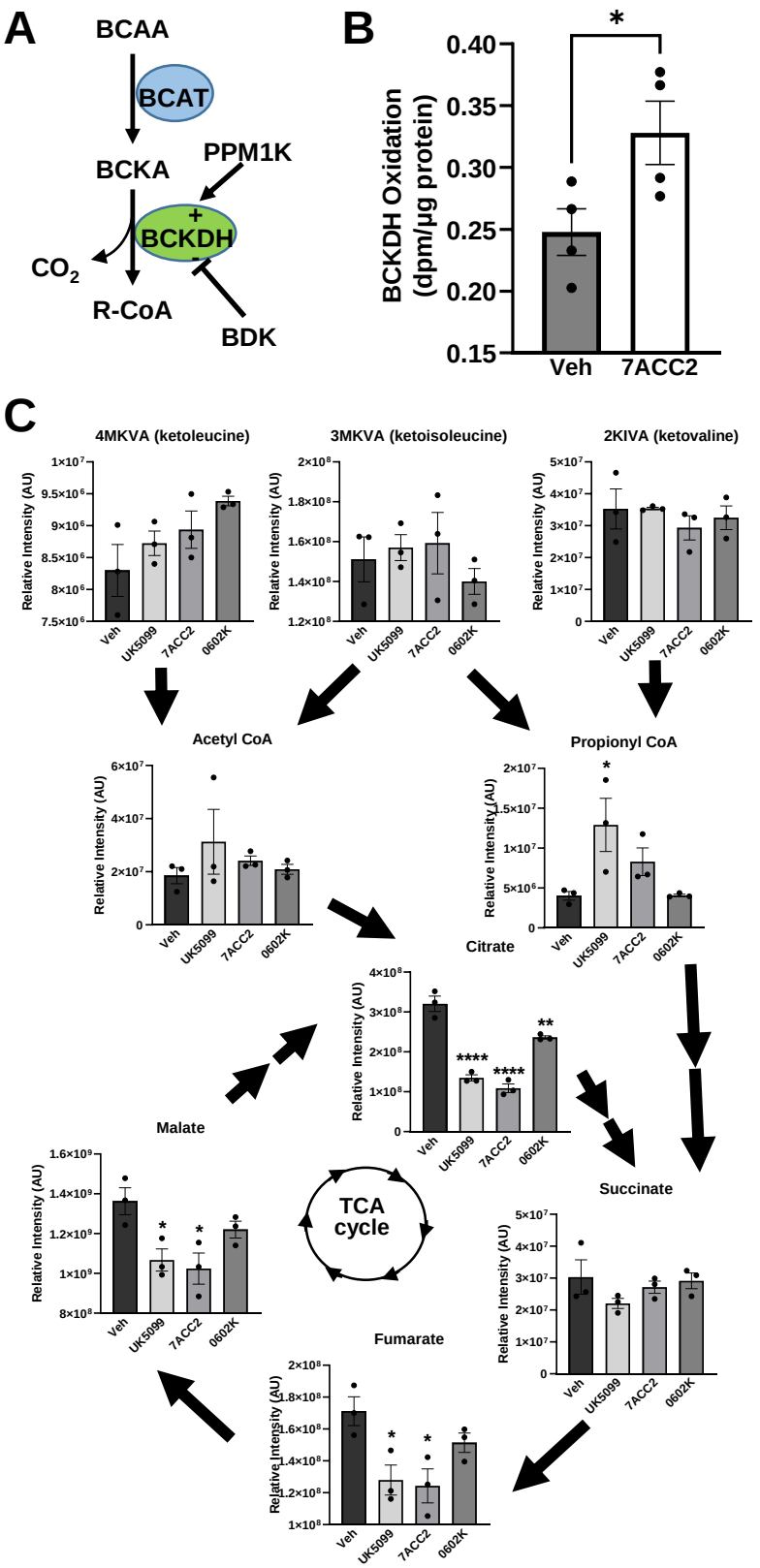

Figure 5

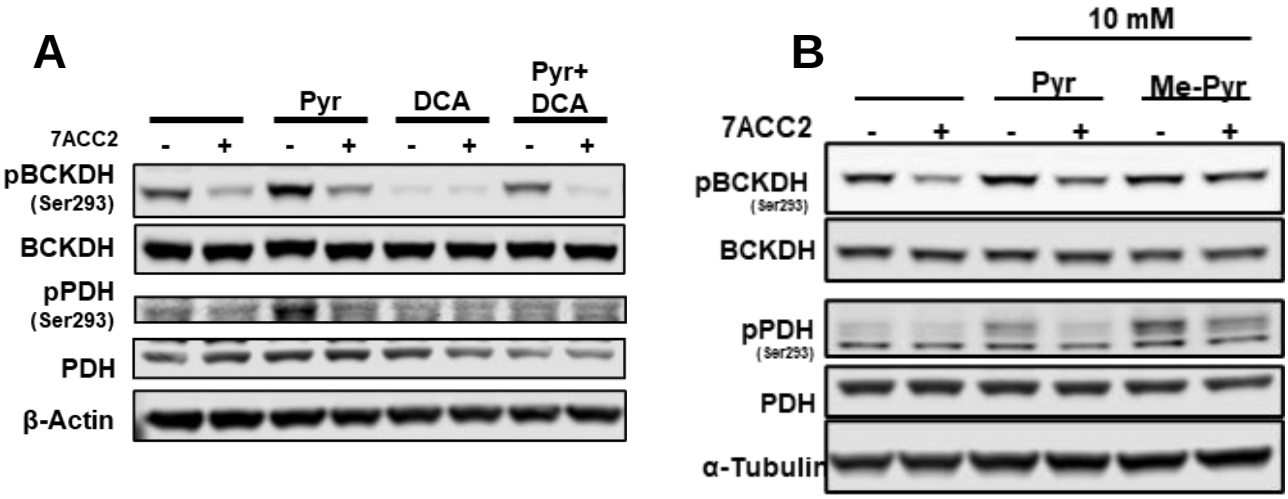

Figure 6

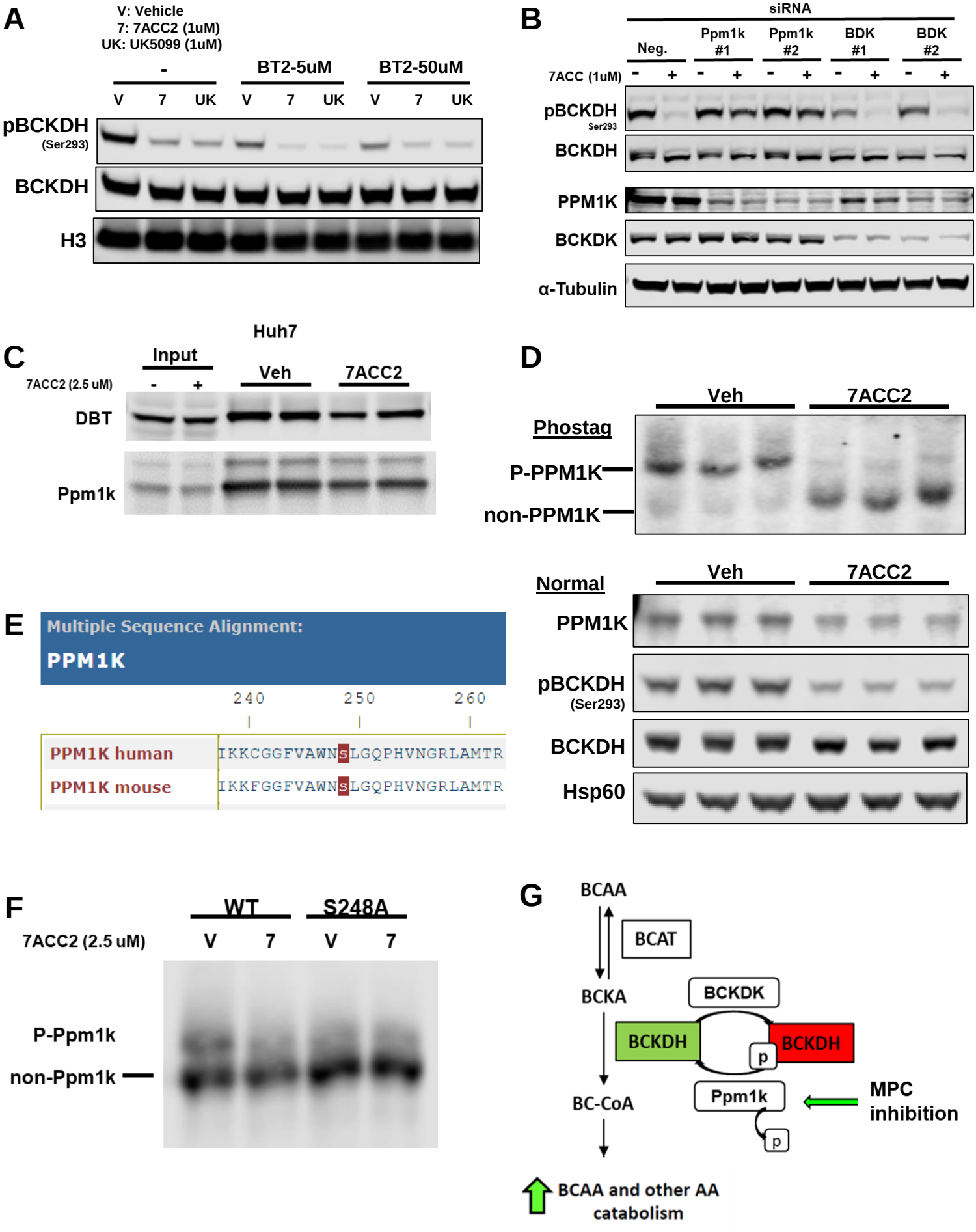

Table 1. Subject characteristics and plasma chemistry

	placebo	low	med	high
Age	54.6 ± 11.2	56.9 ± 10.3	56.0 ± 10.9	56.8 ± 10.4
Sex (M/F)	43/51	43/56	35/63	43/58
N	94	99	98	101
Glucose (mM)				
Mean difference	0.6211 ± 2.344	-0.31 ± 1.744*	-0.5172 ± 2.762*	-0.6759 ± 2.449*
N	76	90	87	87
Insulin (μU/ml)				
Mean difference	2.28 ± 26.99	-2.068 ± 23.47	-6.573 ± 13.87*	-7.601 ± 15.03*
N	75	87	86	82
Adiponectin (ng/ml)				
Mean difference	1796 ± 2017	3038 ± 2982*	4319 ± 4433*	6587 ± 5514*
N	75	90	88	83

Data are means from baseline ± standard deviations; *p<0.05 versus placebo